International Journal of Fatigue 88 (2016) 78–87

Contents lists available at ScienceDirect

International Journal of Fatigue

journal homepage: www.elsevier.com/locate/ijfatigue

# Low-cycle fatigue behaviors of a new type of 10% Cr martensitic steel and welded joint with Ni-based weld metal

Qunbing Zhang [a], Jianxun Zhang [a,*], Pengfei Zhao [b], Yong Huang [b], Zhaohui Yu [a], Xiuyang Fang [a]

[a] *State Key Laboratory for Mechanical Behavior of Materials, Xi'an Jiaotong University, Xi'an 710049, PR China*
[b] *Dongfang Steam Turbine Limited Company, Deyang 618000, PR China*

## ARTICLE INFO

*Article history:*
Received 23 September 2015
Received in revised form 29 February 2016
Accepted 1 March 2016
Available online 8 March 2016

*Keywords:*
Low-cycle fatigue
Welded joint
Ni-based weld metal
Interface

## ABSTRACT

In the present work, Ni-based filler metal was used to weld a new type of 10% Cr martensitic steel. Due to the microstructure and chemical composition difference between martensitic steel and the Ni-based weld metal, a clear interface existed in the dissimilar welded joint. At the region of the interface, the microstructure was physically connected and an element transition layer was formed. Low-cycle fatigue (LCF) results showed that the welded joint was not fractured at the interface. Meanwhile, the martensitic steel and Ni-based weld metal exhibited cyclic softening and cyclic hardening behaviors, respectively. For martensitic steel, the width of the laths increased and the dislocation density decreased after the fatigue test, whereas in the fatigue-tested Ni-based weld metal, the dislocation density increased. The continuous connection and composition transition at the region of interface, combined with the high ductility and cyclic hardening behavior of Ni-based weld metal, is beneficial for the LCF properties of the welded joint.

## 1. Introduction

Because of their good creep property, outstanding corrosion resistance and moderate cost compared to austenitic stainless steels, 9–12% Cr martensitic steels have been extensively used as the structural materials in coal-fired, ultra-supercritical (USC) power plants [1–5].

In response to the problems of environmental pollution and resource depletion, USC power plants with higher specification need to be developed to increase energy efficiency [6–8]. New types of 9–12% Cr martensitic steels with better characteristics are a research hotspot [9–12]. In China, construction of new USC power plants is continuing rapidly [13], and some types of new 9–12% Cr martensitic steels have been developed, such as 12Cr10Co3W2Mo, which is a new type of 10% Cr martensitic steel that was developed based on P92 by increasing the content of Cr and adding 3% Co to improve creep resistance [9,10,13].

However, the welding of 9–12% Cr martensitic steels is a challenge [14,15]. Inadequate welding and post welding processing operations can cause cracks in this class of materials, which can lead to catastrophic failure in operation conditions. Type I–IV creep cracks can manifest in preferential places of the joint [1,16]. The most common one, Type IV cracking, is always leading to premature failure of welded joints compared to the creep life expected from the test of parent steel [17,18]. Therefore, special care must be taken in the welding parameters of this material, such as preheating and inter-pass temperature control, post-weld heat treatment (PWHT), and even more importantly, filler metal.

In the past, the welding of 9–12% Cr martensitic steels frequently used filler materials based on austenitic stainless steels [17,19–21]. From a metallurgical point of view, the austenitic weld metals were problematic due to their susceptibility to solidification cracking. In addition, the creep resistance of these weld joints was found to be rapidly reduced compared to base materials. The main reason for the deteriorated creep strength was attributed to the formation of a soft carbon-depleted zone at the martensitic side of the weld metal interface. To overcome this problem, Ni-based filler metals were introduced. The main benefit of the Ni-based filler metals comes from their low carbon solubility, which makes the filler metals act as a carbon diffusion barrier. Thus, the carbon depletion at the martensitic side of the dissimilar welded joint can be considerably suppressed [22]. Additionally, the high ductility of the Ni-based weld metal can play an important role in the absorption of tensile stress and can decrease the maximum residual stress created during welding, which contributes to the minimization of the crack susceptibility of welded joint [23,24].

The components of USC power plants are often subjected to various damage, such as creep, stress corrosion and fatigue [25].

---

* Corresponding author. Tel.: +86 29 82663115; fax: +86 29 82668807.
*E-mail address:* jxzhang@mail.xjtu.edu.cn (J. Zhang).

http://dx.doi.org/10.1016/j.ijfatigue.2016.03.003
0142-1123/

## Nomenclature

| | |
|---|---|
| LCF | low cycle fatigue |
| $N_f$ | number of cycles to failure |
| $\Delta\varepsilon_t/2$ | total strain amplitude |
| $\Delta\varepsilon_e/2$ | elastic strain amplitude |
| $\Delta\varepsilon_p/2$ | plastic strain amplitude |
| $\Delta\sigma/2$ | stress amplitude |
| $\sigma'_f$ | fatigue strength coefficient |
| $b$ | fatigue strength exponent |
| $\varepsilon'_f$ | fatigue ductility coefficient |
| $c$ | fatigue ductility exponent |
| $R$ | stress ratio |
| $Rz$ | surface roughness |
| PWHT | post-weld heat treatment |

| | |
|---|---|
| BM | base metal |
| WM | weld metal |
| CGWM | columnar-grained weld metal |
| EGWM | equiaxial-grained weld metal |
| HAZ | heat-affected zone |
| CGHAZ | coarse-grained heat-affected zone |
| FGHAZ | fine-grained heat-affected zone |
| ICHAZ | inter-critically heat-affected zone |
| OTHAZ | over-tempered heat-affected zone |
| OM | optical microscopy |
| SEM | scanning electron microscopy |
| EDS | energy dispersive spectrometry |
| TEM | transmission electron microscopy |

System start-ups and shut-downs, as well as power transients, produce repeated low-cycle thermal and mechanical stresses in the components, which has a large impact on safe and reliable operation [20,26–28]. Among all of the damage types, LCF is the most critical for safe and reliable operation [29–31]. At the same time, due to the profound microstructure and chemical composition differences, a clear interface exists in 9–12% Cr martensitic steel, dissimilar welded joint with Ni-based weld metal. The interface is likely to be the weakest region of the welded joint [32–34]. Therefore, it is crucial to study the connectivity of the interface, which is extremely important for determining the LCF properties of the welded joint. Although many studies have investigated the LCF behavior of 9–12% Cr martensitic steel welded joint in recent years [29–31,35–37], there is scarce research on the connectivity of the interface of welded joint. At the same time, as a new type of 9–12% Cr martensitic steel, the LCF ability of 12Cr10Co3W2Mo and its welded joint has not been studied. In the present work, well-formed welded joint was obtained with an ENiCrFe-1 Ni-based alloy-covered electrode. The connectivity of the interface and the LCF behaviors of the new 10% Cr martensitic steel and welded joint were studied.

## 2. Experimental process

### 2.1. Materials and weld manufacture

The base metal studied was 12Cr10Co3W2Mo plate with a size of 280 × 180 × 70 mm$^3$. As shown in Fig. 1, a U-groove was opened on both sides of the plate. The welded joint was prepared by shielded metal arc welding. The chemical compositions and mechanical properties of the 12Cr10Co3W2Mo and electrode (ENiCrFe-1) are shown in Tables 1 and 2. Table 3 shows the welding conditions. When the welding process was complete, PWHT was conducted at 963 ± 10 K for 8 h to prevent the generation of cold cracks of the welded joint. Then, the sample was cooled in air to room temperature. Microstructure observation (Figs. 4–8) and LCF tests were conducted on the PWHT welded joint.

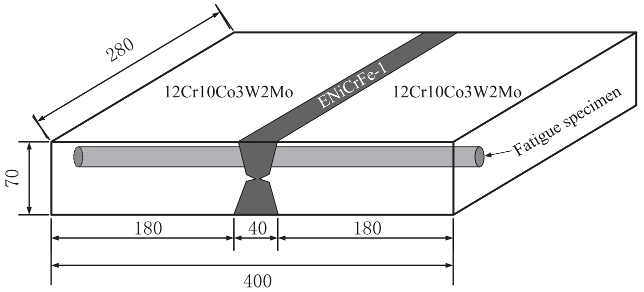

**Fig. 1.** Schematic of the welded joint.

### 2.2. LCF test and microstructure observation

As shown in Fig. 2, LCF tests were conducted on the base metal (BM), weld metal (WM) and the welded joint. The specimen shown in Fig. 2(a) is used to test the strain-life relationship of BM and WM. Fig. 2(b) is the specimen of welded joint, designed to examine the connection ability of the interface. The geometry of fatigue specimen was a cylinder with a uniform gauge section of 8 mm in diameter and 50 mm in length. Prior to the fatigue test, the gauge section was polished to a smooth surface with the surface roughness $Rz = 0.1$. Pull–push (axial) strain-controlled fatigue tests were performed using an electro-hydraulic fatigue machine in atmospheric conditions at room temperature according to the test standard ISO 12106:2003. A triangular waveform was selected with a frequency of 0.25 Hz and a strain ratio of $R = -1$. Different strain amplitudes from 0.4% to 1.2% were chosen.

For different strain amplitudes, three specimens were tested and all of the three fatigue lives were used to decrease experiment error. The number of cycles to failure, $N_f$, was defined as the cycle number at which the maximum stress decreased by 30%. After that, the received specimens were fractured by tensile testing machine. As shown in Fig. 3, the analysis of the cyclic behavior was performed using the following parameters: the total strain range $\Delta\varepsilon_t$, total strain amplitude $\Delta\varepsilon_t/2$; total plastic strain range $\Delta\varepsilon_p$, plastic strain amplitude $\Delta\varepsilon_p/2$; total elastic strain range $\Delta\varepsilon_e$, elastic strain amplitude $\Delta\varepsilon_e/2$ and the stress amplitude $\Delta\sigma/2$.

Optical microscopy (OM) and scanning electron microscopy (SEM) were used to analyze the microstructure, fracture location and fracture morphology of the welded joint. Energy dispersive spectrometry (EDS) and transmission electron microscopy (TEM)

**Table 1**
Chemical composition of 12Cr10Co3W2Mo and ENiCrFe-1 (wt.%).

| Material | C | Mn | Cr | Co | W | V | Mo | Ni | Nb | N | Fe |
|---|---|---|---|---|---|---|---|---|---|---|---|
| 12Cr10Co3W2Mo | 0.11 | 0.08 | 9.82 | 3.06 | 1.72 | 0.20 | 0.71 | 0.36 | 0.08 | 0.03 | Balance |
| ENiCrFe-1 | 0.05 | 3.00 | 16.50 | – | – | – | 0.30 | 70.00 | 2.60 | – | 6.50 |